Resonance-Continuum Interference in the Diphoton Higgs Signal at the LHC

Lance Dixon and M. Stewart Siu

Stanford Linear Accelerator Center, Stanford University, Stanford, California 94309, USA

(Received 25 February 2003; published 23 June 2003)

A low mass standard model Higgs boson should be visible at the Large Hadron Collider through its production via gluon-gluon fusion and its decay to two photons. We compute the interference of this resonant process, $gg \to H \to \gamma\gamma$, with the continuum QCD background, $gg \to \gamma\gamma$, induced by quark loops. Helicity selection rules suppress the effect, which is dominantly due to the imaginary part of the two-loop $gg \to \gamma\gamma$ scattering amplitude. The interference is destructive, but only of order 5% in the standard model, which is still below the 10%–20% present accuracy of the total cross section prediction. We comment on the potential size of such effects in other Higgs models.

DOI: 10.1103/PhysRevLett.90.252001 PACS numbers: 12.38.Bx, 14.70.Bh, 14.80.Bn

The Higgs boson is the lone undetected elementary particle of the standard model (SM), and the only scalar [1]. In the SM, it accounts for the masses of the W and Z bosons, quarks, and charged leptons, and its properties are completely fixed by its mass. Its detection and the measurement of its properties are among the prime goals of the Fermilab Tevatron and the CERN Large Hadron Collider (LHC).

There is a good chance that the Higgs boson will be quite light. Its mass in the SM is bounded from above by precision electroweak measurements, $m_H \lesssim 196$–230 GeV at 95% confidence level [2]. The lightest Higgs boson in the minimal supersymmetric standard model (MSSM) must have a mass below about 135 GeV [3]. These upper limits are not far above the lower bounds established by direct searches in the process $e^+e^- \to HZ$ at the Large Electron Positron Collider (LEP2). The lower bound on the Higgs mass in the SM is 114.1 GeV; it drops to 91.0 GeV in the MSSM because the HZZ coupling can be suppressed [4].

With sufficient integrated luminosity, run II of the Tevatron may be able to discover a low mass Higgs; otherwise the task will fall to the LHC. For $m_H < 140$ GeV, the most important mode at the LHC involves Higgs production via gluon fusion, $gg \to H$ [5], followed by the rare decay into two photons, $H \to \gamma\gamma$ [6,7]. Although this mode has a very large continuum $\gamma\gamma$ background [7,8], the narrow width of the Higgs boson, combined with the 1% mass resolution achievable in the LHC detectors, allows the background to be measured experimentally and subtracted from a putative signal peak [9].

The branching ratio information provided by the $\gamma\gamma$ signal is limited by the accuracy of the cross section for inclusive Higgs production, $\sigma_H \equiv \sigma(pp \to HX)$, because only the product $\sigma_H \times \mathrm{Br}(H \to \gamma\gamma)$ is measured experimentally. The next-to-leading order QCD corrections to σ_H (dominated by gluon fusion) are very large [10]. Recently σ_H was computed at next-to-next-to-leading order (NNLO) [11], in the heavy top quark limit—which is an excellent approximation to the exact NLO cross section [10] for $m_H < 200$ GeV. Threshold logarithms have also been resummed at next-to-next-to-leading logarithmic accuracy [12]. The residual theoretical uncertainties for σ_H, estimated by varying renormalization and factorization scales, are currently of order 10%–20%. [The uncertainty in $\mathrm{Br}(H \to \gamma\gamma)$ is dominated by that in the $H \to b\bar{b}$ partial width and is smaller, of order 6% [13].] In comparison, the anticipated experimental uncertainty in $\sigma_H \times \mathrm{Br}(H \to \gamma\gamma)$ with 100 fb^{-1} of integrated luminosity per LHC detector is about 10% for 115 GeV $< m_H <$ 145 GeV [14].

It is critical to verify that no other physics alters the strength of the $\gamma\gamma$ signal at the 10% level. A potential worry, addressed in this Letter, is the interference between the resonant Higgs amplitude $gg \to H \to \gamma\gamma$ and the continuum $gg \to \gamma\gamma$ scattering process induced by light quark loops. Higgs resonance-continuum interference has been studied previously in $gg \to H \to t\bar{t}$ at a hadron collider [15], and in $\gamma\gamma \to H \to W^+W^-$ and ZZ at a photon collider [16]. These studies assumed that the Higgs boson is heavy enough to have a GeV-scale width. In the case of a light [$m_H < 2\,\min(m_W, m_t)$], narrow-width Higgs boson, the interference in $gg \to H \to \gamma\gamma$ was considered [8], but the dominant contribution in the SM was not identified. Resonance-continuum interference effects are usually tiny for a narrow resonance, and for $m_H < 150$ GeV the width Γ_H is less than 17 MeV. However, the $gg \to H \to \gamma\gamma$ resonance is also rather weak. As shown in Fig. 1, it consists of a one-loop production amplitude followed by a one-loop decay amplitude. Thus a one-loop (or even two-loop) continuum amplitude can partially compete with it.

In the SM, the production amplitude $gg \to H$ is dominated by a top quark in the loop. The decay $H \to \gamma\gamma$ is dominated by the W boson, with some t quark contribution as well. For $m_H < 160$ GeV, the Higgs is below the $t\bar{t}$ and WW thresholds, so the resonant amplitude is mainly real, apart from the relativistic Breit-Wigner factor. The

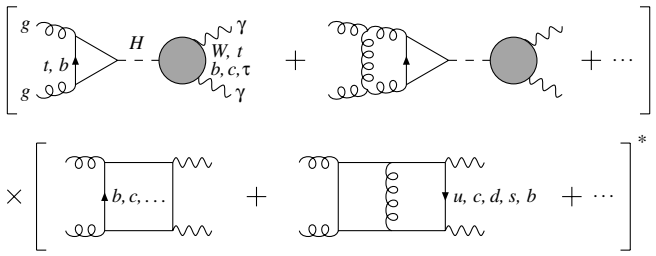

FIG. 1. Sample Feynman diagrams contributing to the interference of $gg \to H \to \gamma\gamma$ with the continuum background. Only one diagram is shown at each loop order, for each amplitude. The blob contains W and t loops and small contributions from lighter charged fermions.

full $gg \to \gamma\gamma$ amplitude is a sum of resonance and continuum terms,

$$\mathcal{A}_{gg\to\gamma\gamma} = \frac{-\mathcal{A}_{gg\to H}\mathcal{A}_{H\to\gamma\gamma}}{\hat{s} - m_H^2 + im_H\Gamma_H} + \mathcal{A}_{\rm cont}, \tag{1}$$

where $\hat{s}$ is the gluon-gluon invariant mass. The interference term in the partonic cross section is

$$\delta\hat{\sigma}_{gg\to H\to\gamma\gamma} = -2(\hat{s} - m_H^2)\frac{\mathrm{Re}(\mathcal{A}_{gg\to H}\mathcal{A}_{H\to\gamma\gamma}\mathcal{A}^*_{\rm cont})}{(\hat{s} - m_H^2)^2 + m_H^2\Gamma_H^2} - 2m_H\Gamma_H\frac{\mathrm{Im}(\mathcal{A}_{gg\to H}\mathcal{A}_{H\to\gamma\gamma}\mathcal{A}^*_{\rm cont})}{(\hat{s} - m_H^2)^2 + m_H^2\Gamma_H^2}. \tag{2}$$

At the hadron level, the interference term is

$$\delta\sigma_{pp\to H\to\gamma\gamma} = \int \frac{d\hat{s}}{\hat{s}}\frac{dL_{gg}}{d\hat{s}}\delta\hat{\sigma}_{gg\to H\to\gamma\gamma}, \tag{3}$$

where the gluon-gluon luminosity function is

$$\frac{dL_{gg}}{d\hat{s}} = \int_0^1 dx_1 dx_2 x_1 g(x_1) x_2 g(x_2)\delta(\hat{s}/s - x_1x_2). \tag{4}$$

The intrinsic Higgs width Γ_H is much narrower than the experimental resolution $\delta m_H \sim 1$ GeV, so the observable interference effect requires an integral across the entire linewidth. The integral of the first, "real," term in Eq. (2) vanishes in the narrow-width approximation [8] and leads to a subdominant effect, to be discussed below.

The second, "imaginary," term in Eq. (2) has the same $\hat{s}$ dependence as the resonance itself, so it survives integration over $\hat{s}$ in the narrow-width limit [not counting the Γ_H factor already explicit in Eq. (2)]. However, it requires a *relative phase* between the resonant and continuum amplitudes. As mentioned above, in the SM the resonant amplitude, apart from the Breit-Wigner factor, is predominantly real. The one-loop continuum $gg \to \gamma\gamma$ amplitude is mediated by light quarks in the loop. Thus one might expect $\mathcal{A}_{\rm cont}$ to have a large imaginary part, which is related by unitarity to the tree amplitude product $\mathcal{A}_{gg\to q\bar{q}} \times \mathcal{A}_{q\bar{q}\to\gamma\gamma}$. For some gluon-photon helicity configurations this is true, but for the like-helicity cases $g^\pm g^\pm$ and $\gamma^\pm\gamma^\pm$ relevant for interference with a scalar Higgs resonance, the tree amplitudes vanish as $m_q \to 0$ [8]. At one loop, the imaginary part of $\mathcal{A}_{\rm cont}$ comes mainly from the b and c quark loops (as indicated in Fig. 1) and is suppressed by factors of order $e_q^2 m_q^2/m_H^2$.

A much larger imaginary part of $\mathcal{A}_{\rm cont}$ arises at the two-loop order, where there is no quark mass suppression [17]. In fact, the imaginary part of the two-loop $gg \to \gamma\gamma$ amplitude is divergent due to an exchange of a soft-collinear virtual gluon between the two incoming gluons, but this divergence cancels against a similar two-loop contribution to the production amplitude $\mathcal{A}_{H\to gg}$. We write the fractional interference correction to the resonance, for polarized gluons and photons, as

$$\delta \equiv \frac{\delta\hat{\sigma}}{\hat{\sigma}} = 2m_H\Gamma_H\mathrm{Im}\Big[\frac{\mathcal{A}^{(1)}_{\rm cont}}{\mathcal{A}^{(1)}_{gg\to H}\mathcal{A}^{(1)}_{H\to\gamma\gamma}} \times\Big(1 + \frac{\mathcal{A}^{(2)}_{\rm cont}}{\mathcal{A}^{(1)}_{\rm cont}} - \frac{\mathcal{A}^{(2)}_{gg\to H}}{\mathcal{A}^{(1)}_{gg\to H}} - \frac{\mathcal{A}^{(2)}_{H\to\gamma\gamma}}{\mathcal{A}^{(1)}_{H\to\gamma\gamma}}\Big)\Big], \tag{5}$$

where for $\hat{s} = m_H^2$ [5,6]

$$\mathcal{A}^{(1)}_{gg\to H} = \sqrt{G_F/2\sqrt{2}}\frac{\alpha_s(m_H)m_H^2}{3\pi}\sum_{q=t,b,c} A_Q(4m_q^2/m_H^2), \tag{6}$$

$$\mathcal{A}^{(1)}_{H\to\gamma\gamma} = \sqrt{G_F/2\sqrt{2}}\frac{\alpha m_H^2}{2\pi} \times\Big(3\sum_{q=t,b,c} e_q^2 A_Q^{\mathcal{H}}(4m_q^2/m_H^2) + A_Q^{\mathcal{H}}(4m_\tau^2/m_H^2) + A_W^{\mathcal{H}}(4m_W^2/m_H^2)\Big), \tag{7}$$

with

$$A_Q(x) = \tfrac{3}{4}A_Q^{\mathcal{H}}(x) = \tfrac{3}{2}x[1 + (1-x)f(x)], \tag{8}$$

$$A_W^{\mathcal{H}}(x) = -x\Big(3 + \frac{2}{x} + 3(2-x)f(x)\Big), \tag{9}$$

$$f(x) = \begin{cases} [\sin^{-1}(1/\sqrt{x})]^2, & x \ge 1, \\ -\frac{1}{4}[\ln(\frac{1+\sqrt{1-x}}{1-\sqrt{1-x}}) - i\pi]^2, & x < 1. \end{cases} \tag{10}$$

Up to constant prefactors, the one-loop continuum amplitude $\mathcal{A}^{(1)}_{\rm cont}$ for $gg \to \gamma\gamma$ is the same as for light-by-light scattering [8,18] and is included with full quark mass dependence. The two-loop amplitude $\mathcal{A}^{(2)}_{\rm cont}$ is evaluated in the $m_q \to 0$ limit [17], after canceling the divergent terms in the ratio $\mathcal{A}^{(2)}_{\rm cont}/\mathcal{A}^{(1)}_{\rm cont}$ against those in $\mathcal{A}^{(2)}_{gg\to H}/\mathcal{A}^{(1)}_{gg\to H}$. The remaining two-loop QCD corrections from $\mathcal{A}^{(2)}_{gg\to H}$ and $\mathcal{A}^{(2)}_{H\to\gamma\gamma}$ are included [19] but are small because they do not induce new phases.

A simplified approximate formula can be given by neglecting the remaining $\mathcal{A}^{(2)}_{gg\to H}$ and $\mathcal{A}^{(2)}_{H\to\gamma\gamma}$ terms, the small phase of $\mathcal{A}^{(1)}_{\rm cont}$, and all but the (real) W and t loops in $\mathcal{A}^{(1)}_{H\to\gamma\gamma}$ and $\mathcal{A}^{(1)}_{gg\to H}$. There are two CP-inequivalent helicity configurations, $g^+g^+ \to \gamma^+\gamma^+$

and $g^-g^- \to \gamma^+\gamma^+$. However, the latter configuration continues to have a vanishing imaginary part at two loops, for massless quarks. In terms of the functions $F^{\rm L}_{--++}$ and $F^{\rm SL}_{--++}$ used in Ref. [17] to describe the former configuration, the correction in the unpolarized case is

$$\delta \approx \frac{2\alpha\alpha_s^2(m_H)m_H\Gamma_H \sum_{q=u,c,d,s,b} e_q^2}{\pi {\rm Re}(\mathcal{A}^{(1)}_{gg\to H}){\rm Re}(\mathcal{A}^{(1)}_{H\to\gamma\gamma})} \times \left(3{\rm Im}F^{\rm L}_{--++}(\theta) - \frac{1}{3}{\rm Im}F^{\rm SL}_{--++}(\theta)\right), \qquad (11)$$

where θ is the $gg \to \gamma\gamma$ center of mass scattering angle.

Figure 2 shows the result of evaluating the unpolarized version of Eq. (5). We let $\alpha = 1/137.036$, $\alpha_s(m_Z) = 0.119$, and use $\overline{\rm MS}$ quark masses evaluated at $\mu = m_H$, with $m_t(m_t) = 164.6$ GeV, $m_b(m_b) = 4.24$ GeV. Our program for Higgs boson decay widths is in good agreement with Ref. [20]. The left panel of Fig. 2 plots δ as a function of m_H, for $\theta = 45°$. The solid curve is the full result, while four other dashed and dotted curves illustrate the result with one source of phase turned on at a time. The effect is dominated by the phase arising from the imaginary part of the two-loop continuum amplitude, for the helicity configuration $g^+g^+ \to \gamma^+\gamma^+$, as given by Eq. (11). Not surprisingly, it is smallest in the region the $\gamma\gamma$ signal is the strongest, 100 GeV $< m_H <$ 140 GeV. As m_H increases toward $2m_W$, the channel $H \to WW^*$ opens up, so Γ_H and hence δ rise rapidly. The large phase arising from $\mathcal{A}_{H\to\gamma\gamma}$ for $m_H > 2m_W$ is visible in the plot; however, such a signal will not be visible at the LHC.

The right panel of Fig. 2 gives the θ dependence of δ for $m_H = 140$ GeV. The imaginary part of the continuum amplitude is forward peaked, so the effect rises there. But the incoherent $q\bar{q} \to \gamma\gamma$ background is also forward peaked, so the experimental searches focus on central scattering angles. Indeed, at $m_H = 140$ GeV, an event with $\theta < 34.9°$ and no gluon radiation will produce photons with transverse momentum $p_{\rm T}(\gamma_{1,2}) < 40$ GeV, below the standard ATLAS and CMS $p_{\rm T}$ cuts [9].

At the same order in α_s as the virtual corrections to $gg \to H \to \gamma\gamma$ represented by Eq. (5), there are radiative corrections from the process $gg \to H \to \gamma\gamma g$ interfering with the one-loop $gg \to \gamma\gamma g$ continuum amplitude induced by light quarks. We evaluate the resonant amplitude in the heavy top approximation (see, e.g., Ref. [21]), neglecting its small absorptive part, and take the absorptive part of the continuum amplitude for five massless quarks [22]. In the unpolarized cross section, only three CP conjugate pairs contribute, due to helicity selection rules. We convolute the interference term with standard gluon distributions and integrate over the final-state gluon momentum numerically, with realistic rapidity and $p_{\rm T}$ cuts on the photons. The result is remarkably miniscule compared to the virtual correction, amounting to 0.01% or less of the signal.

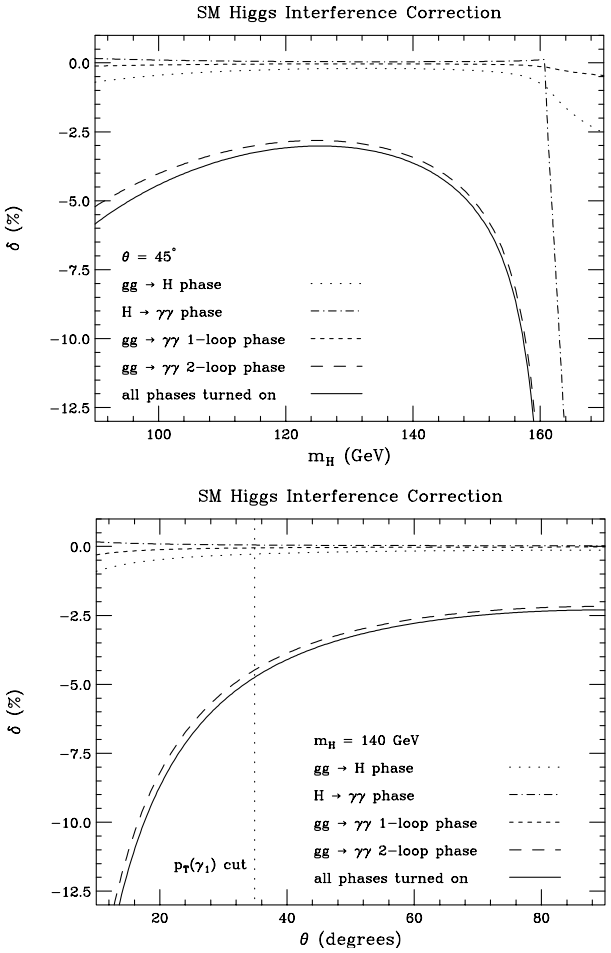

FIG. 2. Top panel: the percentage reduction of the SM Higgs $\gamma\gamma$ signal as a function of the Higgs mass, for the center-of-mass scattering angle $\theta = 45°$. The solid curve gives the result with all phases turned on; the other curves turn on one of the component phases at a time. Bottom panel: the same quantities, plotted as a function of the scattering angle, for $m_H =$ 140 GeV. The vertical dotted line indicates that an event with $\theta < 34.9°$ will not pass the standard ATLAS and CMS photon $p_{\rm T}$ cuts.

Finally, we return to the real term in Eq. (2). It contains the factor $\hat{s} - m_H^2$ which is odd about m_H. The resulting dip-peak structure vanishes under integration [8], provided that the nonresonant functions of $\hat{s}$ vary slowly enough. We perform a first-order Taylor expansion of these functions about m_H, which introduces a linear dependence on the cutoff (mass resolution) into the integral. For a resolution of 1 GeV, the integral of the real term in Eq. (2) is negligible, representing 0.1% or less of the $\gamma\gamma$ signal over the region where it is visible. The contribution rises to a few percent for m_H very near $2m_W$, where $\mathcal{A}_{H\to\gamma\gamma}$ has a sharp energy dependence (which is likely to be smoothed out by finite Γ_W effects). At this large a Higgs mass, however, the $H \to \gamma\gamma$ signal is unobservable.

Nonstandard Higgs sectors or other particle content could in principle generate a larger interference effect. For example, the Higgs coupling to the b quark and τ

lepton can be greatly enhanced in two-Higgs doublet models, including the MSSM. This will increase the size of the phases of $\mathcal{A}_{gg\to H}$ and $\mathcal{A}_{H\to\gamma\gamma}$ in Fig. 2. However, these phases are subdominant to the phase of $\mathcal{A}^{(2)}_{\rm cont}$ in the SM, so the largest effect on Eq. (5) may come from an increase in Γ_H due to the $Hb\bar{b}$ coupling. Yet if Γ_H increases, the $H \to \gamma\gamma$ branching ratio typically decreases, making this mode more difficult to detect and measure accurately. A more quantitative study is in progress [23].

Could other Higgs production and decay processes have appreciable interference effects? At hadron or lepton colliders, the process $gg \to H \to \gamma\gamma$ is almost unique in proceeding only at two loops. The only other potential signal of this type is $gg \to H \to Z\gamma$. The same helicity selection rules prohibit a one-loop continuum phase but allow a two-loop one, so we expect to find an effect of similar magnitude, once the two-loop $gg \to Z\gamma$ amplitude is computed. The photon collider process $\gamma\gamma \to H \to \gamma\gamma$ will be discussed elsewhere; the corrections are below 1% [23]. Returning to the LHC, weak boson fusion followed by $H \to WW^*$ proceeds at tree level. However, the Z resonance can produce a significant phase in the one-loop continuum $W^*W^* \to WW^*$ amplitude, so this case may deserve investigation as well.

In summary, we have computed the dominant continuum interference corrections to the diphoton signal for the standard model Higgs boson produced via gluon fusion. The effects are at the 2%–6% level, depending on the Higgs mass and scattering angles. While still small compared to present theoretical and anticipated experimental errors, they are not totally negligible and suggest that further study is warranted of similar effects in nonstandard models and for other selected channels.

We are grateful to Zvi Bern for suggesting this work. We also thank Stefano Catani, Howard Haber, Maria Krawczyk, Zoltan Kunszt, Stefano Moretti, Michael Peskin, and Dieter Zeppenfeld for helpful discussions. This research was supported by the U.S. Department of Energy under Contract No. DE-AC03-76SF00515.

[1] P.W. Higgs, Phys. Lett. **12**, 132 (1964); Phys. Rev. **145**, 1156 (1966); F. Englert and R. Brout, Phys. Rev. Lett. **13**, 321 (1964); G.S. Guralnik, C.R. Hagen, and T.W. Kibble, Phys. Rev. Lett. **13**, 585 (1964).

[2] G. Degrassi, hep-ph/0102137; J. Erler, hep-ph/0102143; ALEPH, DELPHI, L3, and OPAL Collaborations, LEP Electroweak Working Group, and SLD Heavy Flavor and Electroweak Groups, D. Abbaneo *et al.*, hep-ex/0112021.

[3] M. Carena, H.E. Haber, S. Heinemeyer, W. Hollik, C.E. Wagner, and G. Weiglein, Nucl. Phys. **B580**, 29 (2000); J.R. Espinosa and R. Zhang, Nucl. Phys. **B586**, 3 (2000); A. Brignole, G. Degrassi, P. Slavich, and F. Zwirner, Nucl. Phys. **B631**, 195 (2002).

[4] ALEPH Collaboration, R. Barate *et al.*, Phys. Lett. B **495**, 1 (2000); DELPHI Collaboration, P. Abreu *et al.*, Phys. Lett. B **499**, 23 (2001); L3 Collaboration, M. Acciarri *et al.*, Phys. Lett. B **508**, 225 (2001); OPAL Collaboration, G. Abbiendi *et al.*, Phys. Lett. B **499**, 38 (2001); LEP Higgs Working Group for Higgs Boson Searches, hep-ex/0107029; hep-ex/0107030.

[5] H.M. Georgi, S.L. Glashow, M.E. Machacek, and D.V. Nanopoulos, Phys. Rev. Lett. **40**, 692 (1978).

[6] J.R. Ellis, M.K. Gaillard, and D.V. Nanopoulos, Nucl. Phys. **B106**, 292 (1976); M.A. Shifman, A.I. Vainshtein, M.B. Voloshin, and V.I. Zakharov, Sov. J. Nucl. Phys. **30**, 711 (1979) [Yad. Fiz. **30**, 1368 (1979)].

[7] J.F. Gunion, P. Kalyniak, M. Soldate, and P. Galison, Phys. Rev. D **34**, 101 (1986); R.K. Ellis, I. Hinchliffe, M. Soldate, and J.J. van der Bij, Nucl. Phys. **B297**, 221 (1988); J.F. Gunion, G.L. Kane, and J. Wudka, Nucl. Phys. **B299**, 231 (1988).

[8] D.A. Dicus and S.S.D. Willenbrock, Phys. Rev. D **37**, 1801 (1988).

[9] ATLAS Collaboration, "ATLAS Detector and Physics Performance, Technical Design Report," CERN Report No. CERN/LHCC 99-15, ATLAS-TDR-15, 1999; CMS Collaboration, G.L. Bayatian *et al.*, "CMS: The Electromagnetic Calorimeter, Technical Design Report," CERN Report No. CERN/LHCC 97-33, CMS-TDR-4.

[10] A. Djouadi, M. Spira, and P.M. Zerwas, Phys. Lett. B **264**, 440 (1991); S. Dawson, Nucl. Phys. **B359**, 283 (1991); M. Spira, A. Djouadi, D. Graudenz, and P.M. Zerwas, Nucl. Phys. **B453**, 17 (1995).

[11] R.V. Harlander and W.B. Kilgore, Phys. Rev. Lett. **88**, 201801 (2002); C. Anastasiou and K. Melnikov, Nucl. Phys. **B646**, 220 (2002).

[12] S. Catani, D. de Florian, and M. Grazzini, J. High Energy Phys. 05 (2001) 025; M. Grazzini, hep-ph/0209302.

[13] A. Djouadi, M. Spira, and P.M. Zerwas, Z. Phys. C **70**, 427 (1996).

[14] D. Zeppenfeld, R. Kinnunen, A. Nikitenko, and E. Richter-Was, Phys. Rev. D **62**, 013009 (2000).

[15] D. Dicus, A. Stange, and S. Willenbrock, Phys. Lett. B **333**, 126 (1994).

[16] D.A. Morris, T.N. Truong, and D. Zappala, Phys. Lett. B **323**, 421 (1994); P. Niezurawski, A.F. Zarnecki, and M. Krawczyk, J. High Energy Phys. 11 (2002) 034.

[17] Z. Bern, A. De Freitas, and L.J. Dixon, J. High Energy Phys. 09 (2001) 037.

[18] V. Constantini, B. De Tollis, and G. Pistoni, Nuovo Cimento A **2**, 733 (1971); L. Ametller, E. Gava, N. Paver, and D. Treleani, Phys. Rev. D **32**, 1699 (1985).

[19] M. Spira, Fortschr. Phys. **46**, 203 (1998).

[20] A. Djouadi, J. Kalinowski, and M. Spira, Comput. Phys. Commun. **108**, 56 (1998).

[21] R.P. Kauffman, S.V. Desai, and D. Risal, Phys. Rev. D **55**, 4005 (1997); **58**, 119901(E) (1998).

[22] Z. Bern, L. Dixon, and D.A. Kosower, Phys. Rev. Lett. **70**, 2677 (1993); D. de Florian and Z. Kunszt, Phys. Lett. B **460**, 184 (1999); C. Balazs, P. Nadolsky, C. Schmidt, and C.-P. Yuan, Phys. Lett. B **489**, 157 (2000).

[23] L. Dixon and M.S. Siu (to be published).